Hindawi
Advances in Civil Engineering
Volume 2023, Article ID 7563415, 16 pages
https://doi.org/10.1155/2023/7563415

Research Article

Mechanical Analysis of Junction Pier of Fuzhou-Xiamen High-Speed Railway Rigid-Frame Bridge

Fangwen Weng and Fuxing Liu

CCCC Second Harbor Engineering Company Ltd., Wuhan 430040, China

Correspondence should be addressed to Fangwen Weng; sponerock@hbut.edu.cn

Received 2 October 2022; Revised 15 November 2022; Accepted 22 March 2023; Published 24 April 2023

Academic Editor: S. Mahdi S. Kolbadi

The continuous rigid structure bridge on both sides of the Quanzhou Bay Crossing Bridge uses double-limbed thin-walled flexible piers for the junction piers between the links, and the whole bridge has no bearings. In China, the monolithic bearing-free prestressed concrete continuous rigid-frame bridge is used in railway bridges. The junction pier between the two adjacent couplets is a double-leg thin-walled flexible pier. The single leg thin-walled pier is connected with half of the pier-top segment. During the construction process, the block with numbered zero on the top of the pier is temporarily anchored and connected. Symmetrical cantilevered baskets are used on both sides for construction, and after the mid-pier cantilevered construction is completed, the temporary anchoring device for the block with numbered zero is removed. Because the structural system conversion is required in the construction, the mechanical properties of the junction pier will change greatly before and after the conversion, so it is very necessary to calculate and analyze it to master. In this paper, the finite element model of the connecting pier is established accurately, the stress and deformation of each part of the connecting pier under unfavorable working conditions is analyzed in detail, the seismic spectrum analysis under the action of common earthquake and rare earthquake is carried out, and the stress and deformation law of the structure is expounded, which can provide some reference for the construction of similar projects in the future.

1. General Situation of the Project

1.1. Introduction to Rigid Bridge Intersection Piers. The approach bridge on both sides of the main bridge of Fuzhou-Xiamen high-speed railway is an integral bearing-free prestressed concrete continuous rigid-frame bridge. The continuous rigid structure bridge on both sides of the Quanzhou Bay Crossing Bridge uses double-limbed thin-walled flexible piers for the junction piers between the links, and the whole bridge has no bearings. In China, the monolithic bearing-free prestressed concrete continuous rigid-frame bridge is used in railway bridges. The structure of the grouted mortise-tenon joints used in the prefabricated structure is complicated, and the force applied to them is special, but there was very little research on these joints before [1].

The thickness of the box girder roof of the zero block of the connecting pier is gradually changed from 90 cm to 40 cm, and the pier-top segment and the pier body are consolidated with the thick bottom plate. The structure is basically the same as the zero block of the middle pier, except that there is a beam joint in the center of the box girder and the design theoretical width is 15 cm.

The total length of block zero is 12 m, the height of the beam tapers from 660 cm to 607.5 cm, the thickness of the web of block zero tapers from 90 cm to 70 cm, and the thickness of the outer web is increased to 100 cm where it meets the pier. 1.9 m thick cross partitions are provided at the end of the box girder and two 160 cm × 140 cm manholes are provided at each end, the thickness of the bottom plate tapers from 1.5 m to 1.051 m, and water drainage holes are

provided (the flood effect is considered in this element [2]). The thickness of the base plate is gradually changed from 1.5 m to 1.051 m, and drainage holes are provided. The structure of the zero block of the junction pier is shown in Figure 1.

1.2. Anchorage Prestressing of the Zero Block of the Transfer Pier. Common manipulators include rigid manipulators and flexible manipulators. Flexible joint manipulators have significant advantages over traditional rigid manipulators in terms of response speed, control accuracy, and load-to-weight ratio, but they are highly nonlinear and strongly coupled, which brings great challenges to the controller design [3]. The anchorage prestressing in the zero block of the junction pier includes permanent prestressing and temporary prestressing.

The permanent prestressed tendons ST1, ST1, and ST2 use 15 φ^j 15.24 steel strands, while SB1′, SB2′, SB3′, SB5, SB6, and SB7 use 19 φ^j 15.24 steel strands. The layout of permanent prestressed tendons is shown in Figure 2.

The overhanging sections of the junction pier are set up with 2 bundles of SB1′, SB2′, and SB3′ in the corresponding webs from M1 to M8, 4 bundles of SBS and a spare east bundle of SBY in the M1 section of the bottom plate, 4 bundles of SB4 in the M2 section, 2 bundles of SB3 in the M3 section, 4 bundles of SB2 in the M4 section, and 4 bundles of SB1 in the M5 section. The arrangement of prestressing steel bundles in the overhanging sections of the junction pier is shown in Figure 3.

The setting of temporary anchoring prestress can reduce the amount of cast-in-place support and improve the construction efficiency in the construction of rigid-frame bridge. Except for the cast-in-place support for block zero of the transfer pier, the hanging basket cantilever casting technology is adopted for other beam sections. In order to ensure the smooth implementation of the suspension casting construction, the temporary prestress is designed to be set on the transfer pier.

Under the influence of the beam joint at the top of the pier, in order to ensure the construction safety of the cantilever segment, the zero block is temporarily anchored so that the segments on both sides of the beam joint of the zero block form an integral joint. The temporary anchoring of Block Z includes anchoring of the partition plate, as well as anchoring of the top and bottom plates. PSB830φ25 precision-rolled threaded steel is used for the temporary anchoring of the partition plate, which is horizontally and longitudinally anchored on both sides of the beam joint. The stress during anchoring and tension control is 740MPa. The finished rolled rebar is located on and below the manhole, with a total of 4 rows. There are 24 vertical spacing 80 cm and horizontal spacing 40 cm in the upper 2 rows of the manhole and 24 vertical spacing 57 cm and 40 cm horizontal spacing in the lower 2 rows of the manhole, as shown in Figure 4.

The transverse distance between the permanent prestressed steel beam and the temporary prestressed steel beam at the roof is 25 cm. The distance between them is 69 cm at the floor. The web spacing is 80 cm and 55 cm, respectively.

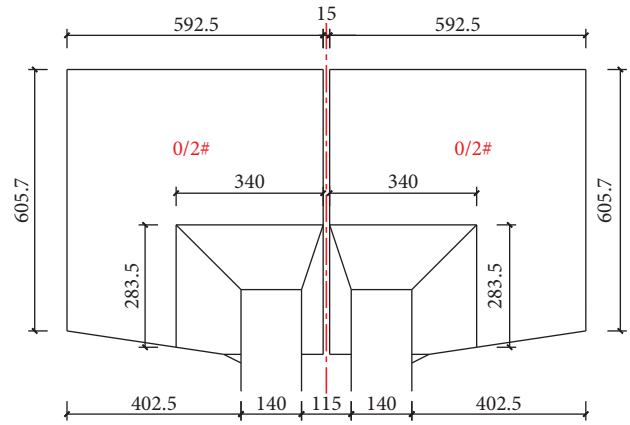

Figure 1: Schematic diagram of the structure of the No. 0 block of the junction pier.

The relative relationship between temporary prestress and permanent prestress is shown in Figure 4.

1.3. Transverse Limiting Device. In order to ensure that the final bridge line type meets the requirements of design and construction technical specifications, transverse limiters are installed at the end of the beam between two pairs of 3×70 m rigid frame and between 3×70 m rigid frame and 2×70 m rigid frame, and each transfer pier has two sets. The transverse limiter is installed in the reserved slot at the end of the beam. The height of the groove is 67 cm and the length is 82 cm. The structure and installation position of the lateral limiter are shown in Figure 5.

2. Key Construction Technology of No. 0 Block of Junction Pier

After the bracket is precompressed, the side formwork, end formwork, and beam seam formwork of the box girder are installed, and then, the bottom web reinforcement and prestressed metal bellows are installed. Then, the inner cavity scaffold is set up, and the inner roof formwork, roof reinforcement, and precast box girder concrete are installed. The relevant construction process of "No. 0 block" of junction pier is shown in Figure 6.

2.1. Installation and Fixing of Beam Seam Formwork. Through the experimental study of six kinds of beam joint support methods (Figure 5), it is found that using 10 mm steel plate as plane formwork and 2.21 mm visa plates as beam joint support has the best mechanical properties and the smallest deformation. The support mode of this kind of beam joint is adopted in the actual construction.

The beam joint support method is to install the prestressed groove template at the bottom plate first, then install the plane template, and finally, install the remaining groove and manhole template in place in turn. The two Vesar plates are fixed with M5 × 60 cross-groove self-tapping screws, and processed in blocks. During processing, holes are opened at the corresponding prestressed pipeline position. After the

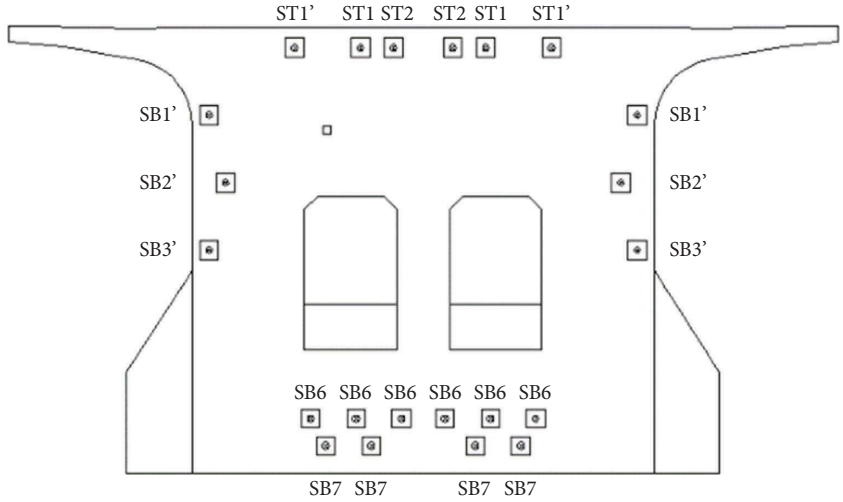

Figure 2: Permanent prestressing layout.

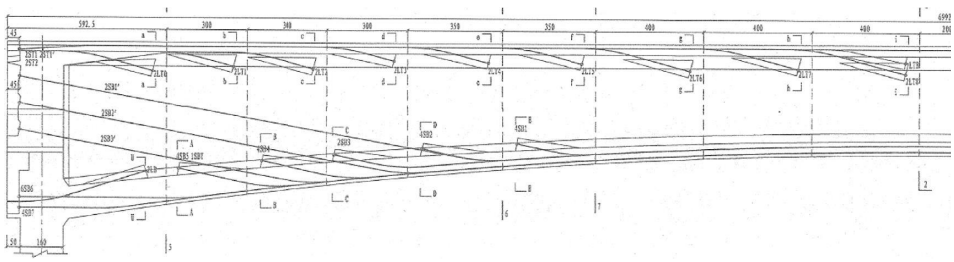

Figure 3: Layout diagram of prestressed steel tendons for cantilever casting segments of junction piers.

assembly of the bottom dies and side die of the zero block is completed, the whole lifting is carried out. The beam seam template is overall located on the bottom die as shown in Figure 7.

tIn nonlinear finite element analysis, it is necessary to have the right assumption of the nonlinear behavior of prestressed reinforced concrete (PC), such as cracking and plasticity of concrete, yielding of reinforcing steel, tension stiffening, and shear retention [4]. After the installation of the beam joint formwork is completed, one end of the equal angled steel with 50 degree is welded on both sides of the steel skeleton, and the other end is used to hold the formwork. The top of the formwork is welded on the side formwork to fix the formwork to prevent the beam joint formwork from floating during the concrete pouring process. The concrete pouring process should be controlled at all times.

The construction of the zero block of the transfer pier is completed, only the reserved slot and the hole template are removed, and the construction of the closure section corresponding to the transfer pier and the adjacent middle piers on both sides is completed in accordance with the construction closure sequence. After all the prestress is tensioned according to the design drawings, the temporary anchorage prestress of the zero block of the transfer pier is lifted, the prestressed pipeline is cut off, and the plane template of the beam joint and the beam support are removed by the Visa plate.

2.2. Prestress Construction. After the construction of the transfer pier-top section and each cantilever section is completed, the concrete strength reaches 95% of the design strength, and the elastic modulus reaches 100% of the design value, and the tension is carried out after the age is not less than 5 days. Tension 2LT0, 2LB, tension control stress of steel strand tension is 1,280 MPa, tension control stress of finishing rolled rebar is 740 MPa, temporary prestressed rebar and temporary prestressed steel strand hole are not grouted. In the construction process, with the prestress tension of each section, the section stress at the beam joint increases gradually, and the increase of the compression of the beam joint support may lead to the relaxation of the temporary prestress. Therefore, the temporary prestress should be checked after the completion of the construction of each section, and the relaxation of the prestressed steel strand or the finishing rolled screw steel should be supplemented.

The permanent prestress tension adopts 450T hydraulic jack, the size is A472 × 374 mm, and the stroke is 200 mm. The prestressed cable at the roof is tensioned by putting the bridge deck into the jack, and the prestressed cable at the floor is tensioned by putting the jack into the manhole. When the prestressed cable at the web is tensioned, 5 cm holes are reserved at the prestressed cable corresponding to the beam joint template, and the jack is fixed and tensioned by the wire rope, as shown in Figure 8.

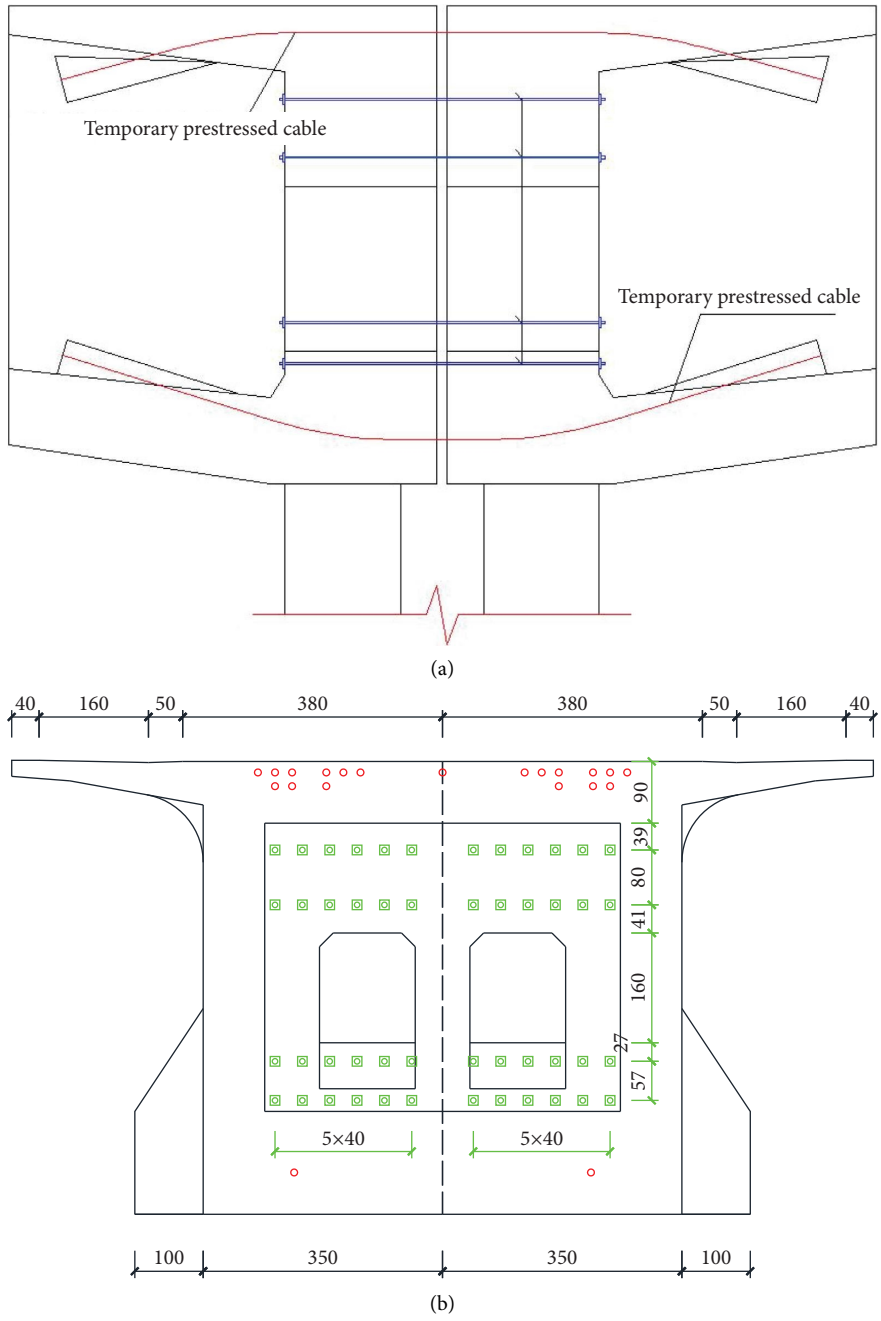

Figure 4: Schematic diagram of the temporary Anchorage structure of the junction pier.

3. Finite Element Analysis

The structure of the transfer pier is more complex and the modeling is more difficult. If the model is established according to the real structure, it will cause abnormal grid division, resulting in nonconvergence of calculation or inaccurate settlement results, so it is necessary to simplify the model. However, this will greatly reduce the reality of the model and reduce the credibility of the analysis results. In this paper, due to the use of the advanced BIM modeling technology (as shown in Figure 9), the parameterized method is used to optimize the model, and the best meshing result is obtained on the basis of not significantly simplifying the model, which not only satisfies the reality of the model but also makes the finite element calculation proceed smoothly. For the mechanical analysis work in the structural design phase, data conversion and information transfer between the BIM model and finite element model have become the main factors limiting its efficiency and quality, with the development of the BIM technology application in the whole life cycle [5].

The high mesh quality of the finite element model and the lack of excessive simplifications improve the confidence of the computational analysis and speed up the finite element solution.

Figure 5: Visa plate compression test.

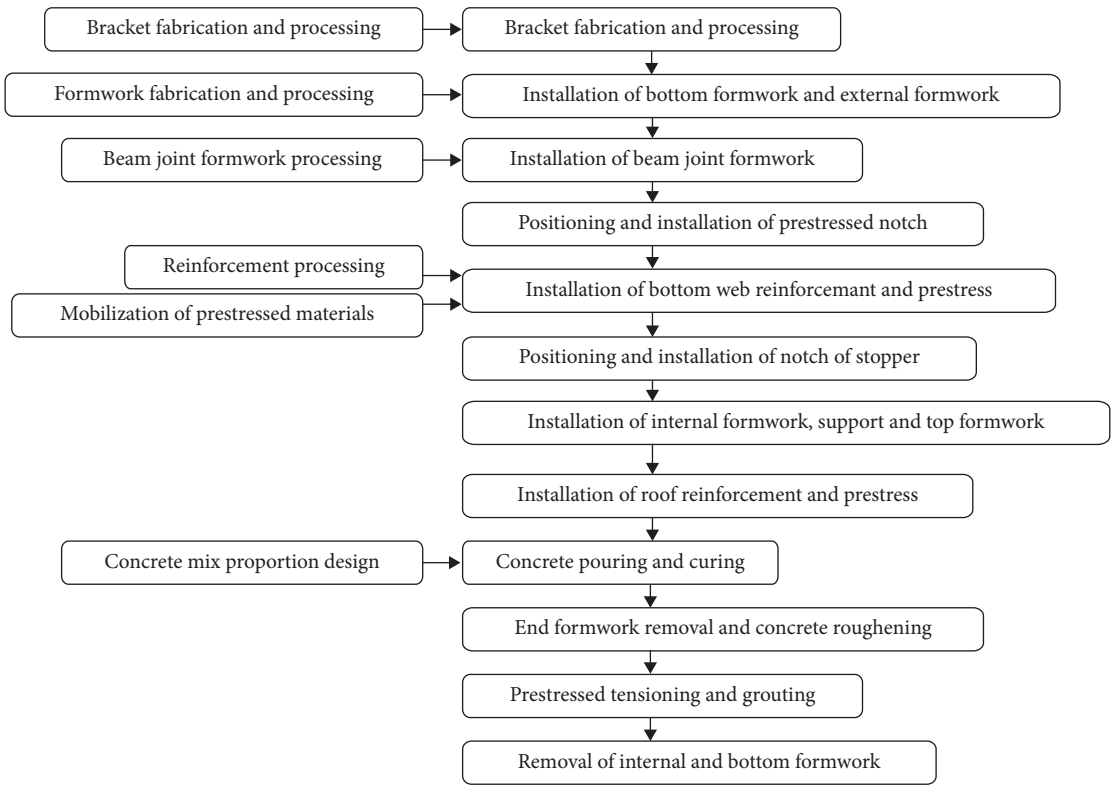

Figure 6: Construction flowchart of No. 0 block of junction pier.

3.1. Finite Element Modelling. In this paper, ABAQUS general finite element analysis software is used for numerical calculation, and the three-dimensional model optimized by the BIM technology is directly imported into the finite element software for meshing. The three structures will interact in the calculation and analysis, namely, the concrete structure of the transfer pier, the beam-slit support structure composed of Visa plate and steel plate, and the permanent and temporary prestressed anchorage system. In order to make the calculation and analysis more accurate, the finite element model truly restores the size and position of the three components, as shown in Figure 10.

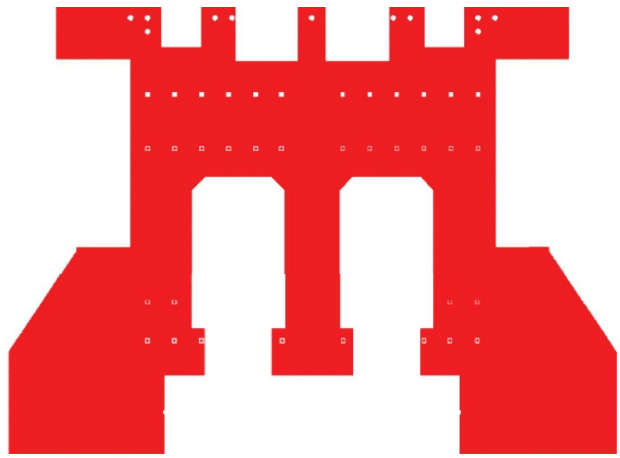

Figure 7: Processing schematic of beam seam template.

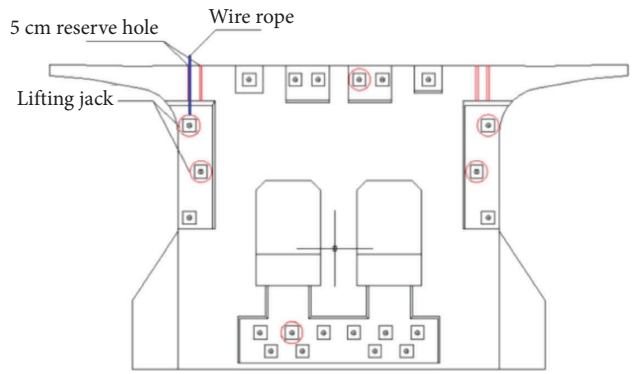

Figure 8: Layout of temporary prestressed tensioned jacks.

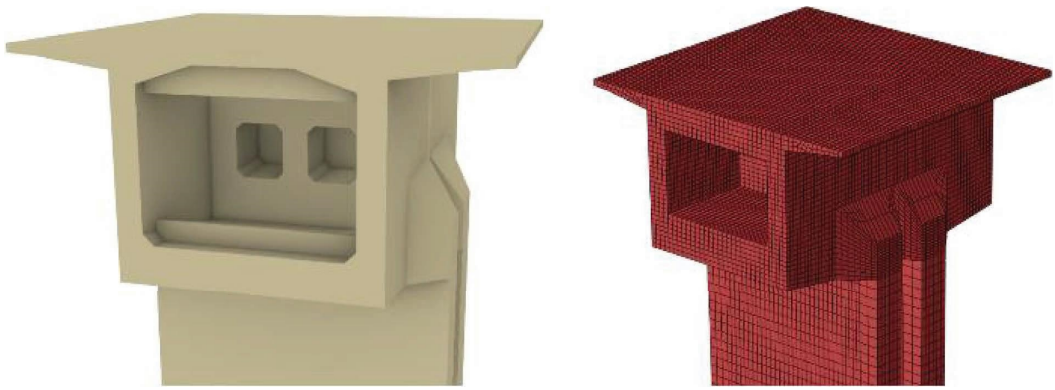

Figure 9: The BIM model and finite element model.

The object of calculation and analysis in this paper is No. 85 connecting pier. The height of the pier is 49.264 m and the height of both legs is 30 m, which is one of the highest three connecting piers. The connecting pier and Visa plate adopt solid element, and the steel bundle adopts cable element, with a total of 128,337 elements and 146,959 nodes. The cable element is embedded in the solid element, and the fixed boundary conditions are set on the bottom of the cap, and the material properties are shown in Table 1.

Before the analysis of the transfer pier, the beam element model is used to calculate and analyze the cantilever construction stage of the transfer pier, and the deformation on both sides of the transfer pier in each construction stage is obtained, which is applied as a boundary condition to the two ends of the solid element model of the transfer pier. Each deformation represents a construction stage. After the construction of block zero of the transfer pier is completed, the cantilever construction shall be continued on both sides

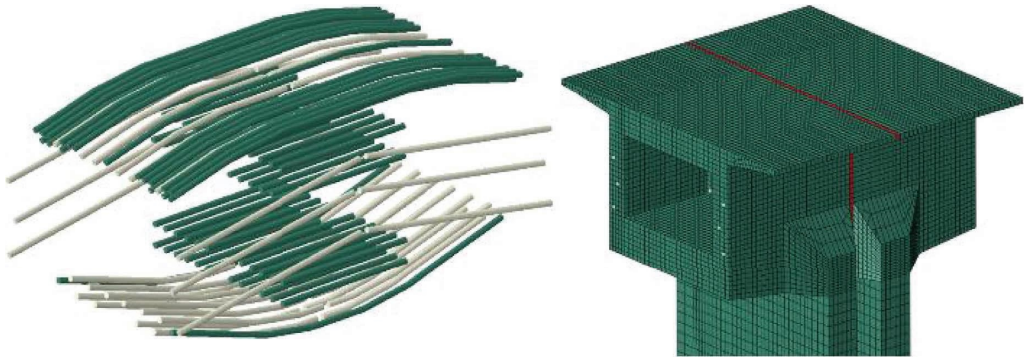

Figure 10: Prestressed steel beam and the Visa plate.

Table 1: Material properties.

Materials	Density (kg/m^3)	Elastic modulus (GPa)	Poisson's ratio
C50 concrete	2,500	35	0.2
Visa board	780	7.6	0.15
Steel products	7850	210	0.25

until the nine construction stages of the closure are shown in Figure 11 and Table 2.

3.2. Static Result Analysis. Due to the temporary anchorage of the zero blocks, it is equivalent to the rigid frame pier in the construction process before closure. The construction load mainly depends on the temporary prestressed steel beam and the finish rolling rebar. The tension control stress of the steel strand is 1,280 MPa, and the tension control stress of the finish rolling rebar is 740 MPa. In the calculation, the controlled prestress construction is applied by changing the temperature load of the material. The stress state before concrete closure is consistent with the middle pier of the rigid-frame bridge, and the deformation is shown in Figure 12.

It can be seen from the figure that due to the application of temporary anchorage prestress, the part of the structure is in a compression state, and the local concrete near the application of prestress has complex stress and large stress. As can be seen from the figure, due to the application of temporary anchorage prestress, the part of the structure is in a state of compression, and the local concrete near the prestress is complex, and there is a large stress. The time-frequency characteristics of the longitudinal displacements of bearings and expansion joints are analyzed using the empirical wavelet transform. The long-term characteristics of the longitudinal displacements of bearings and expansion joints in the operation period are explored [6].

Figure 13 shows the deformation diagram of the prestressed steel bundle and fine threaded steel bar in the second stage of construction. It can be seen that due to the application of prestress, the deformation of steel bundle and rebar is only about 1 mm.

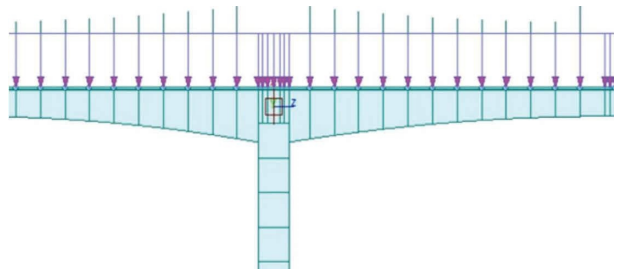

Figure 11: Calculation of the integral construction stage of the beam element model.

Table 2: Deflection of zero blocks in each construction stage.

Construction stage	Deflection (mm)
0	3.1
1	4.9
2	6.2
3	7.8
4	9.3
5	10.8
6	11.6
7	12.2
8	13.1
9	11.5

Note. Construction stage 9 is the closure stage.

As shown in Figure 14, the compressive stress of the visa plate shows an uneven distribution, the maximum compressive stress at the bottom corner is 17 MPa, and the distribution of the compressive stress is related to the size and position of the prestress. The static bending extrusion strength of the Visa plate with the thickness of 21 mm is 25 MPa, and the selected Visa board can meet the requirements of force and deformation.

As can be seen from the left picture of Figure 15, in the cantilever construction, the top of the zero block pier is anchored, the flexible pier will retract from the upper part with the deformation of the zero block, the lower part expands outward with the reverse bending point, and the maximum deformation of the upper part is 9.3 mm. As can be seen from the picture on the right of Figure 15, when the flexible pier is deformed, the tensile stress at the root of the

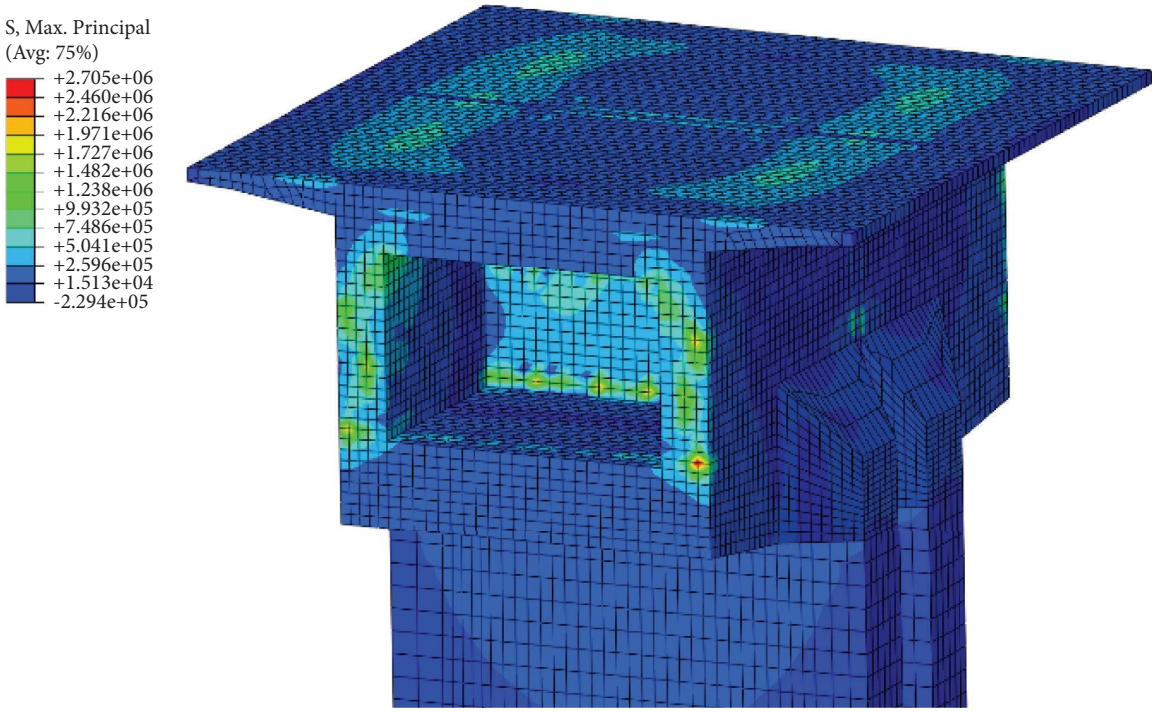

Figure 12: Cloud picture of the second maximum principal stress at the construction stage.

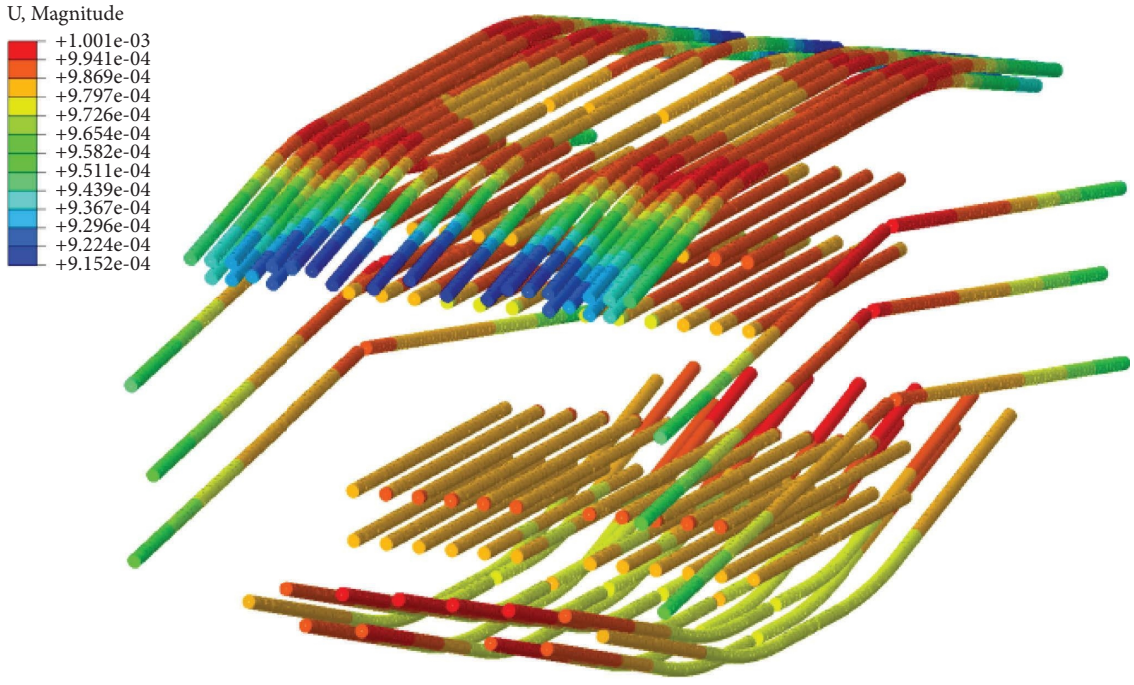

Figure 13: Cloud diagram of deformation of second steel bundle and steel bar in construction stage.

flexible pier is larger, because the internal prestress of the pier is not taken into account in the calculation, the result is only for reference and needs to be locally strengthened at the root of the two limbs.

Figure 16 shows the force and deformation of the connecting pier after the bridge is closed and the anchorage is removed. It can be seen from the figure that due to the release of the constraint at the top of the pier, the loaded piles of the two single limbs are similar to the cantilever beam, and the inside of the single limb is subjected to tensile stress, the maximum tensile stress is about 2.7 MPa, and the maximum deformation of the limb is 33.5 mm. The flexible pier can release the deformation caused by the joint through its own deformation, so as to improve the stress conditions of the

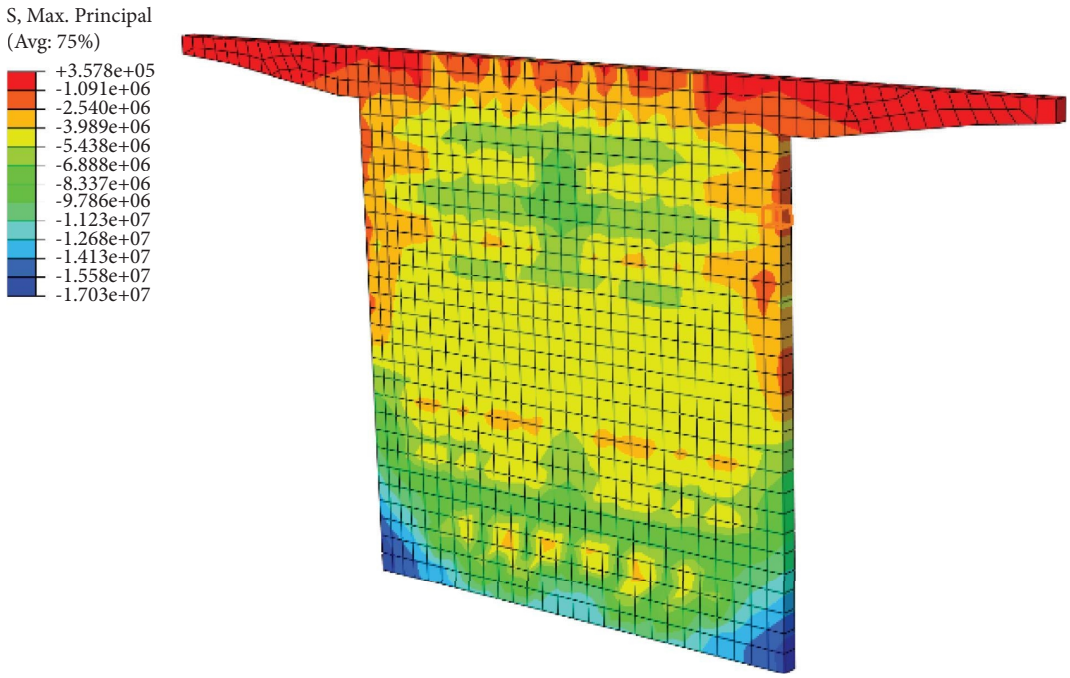

Figure 14: Compressive stress cloud diagram of the Visa plate.

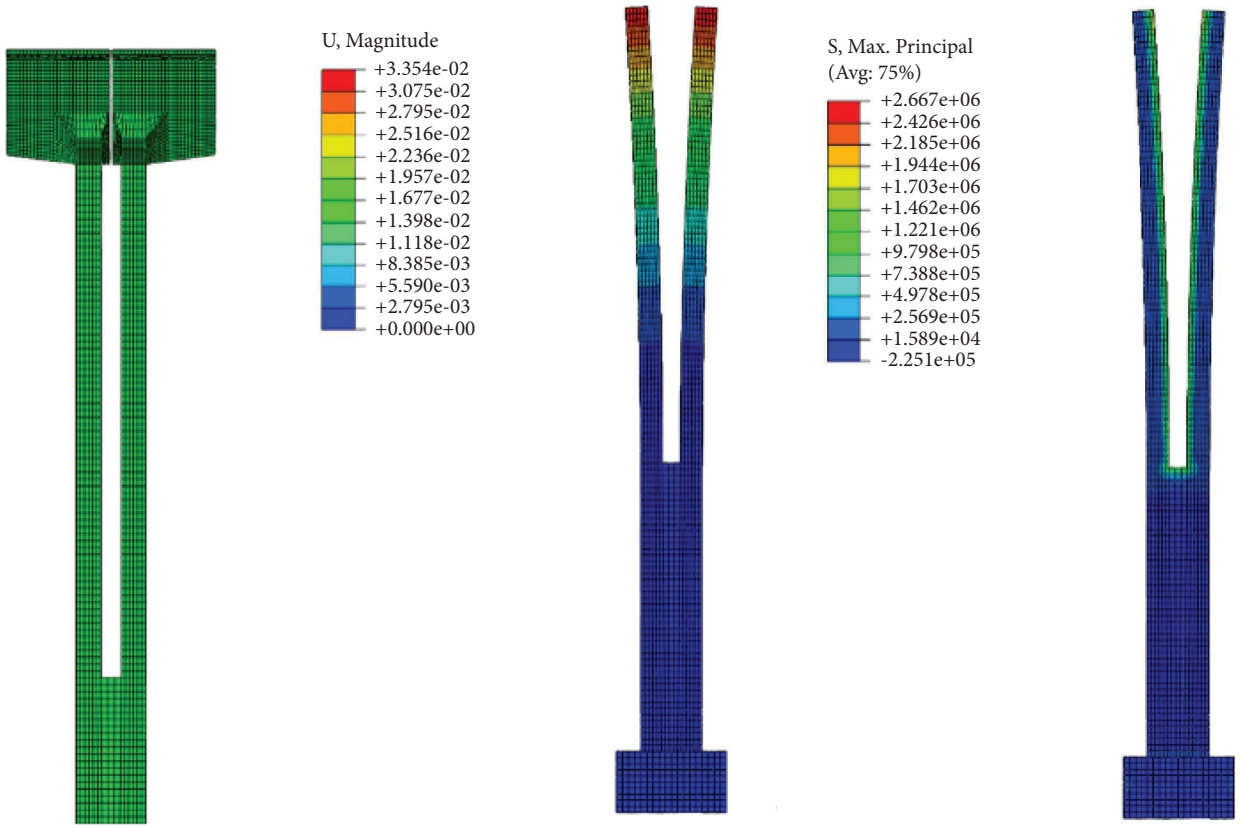

Figure 15: Deformation diagram of double-leg thin-walled piers under anchorage condition.

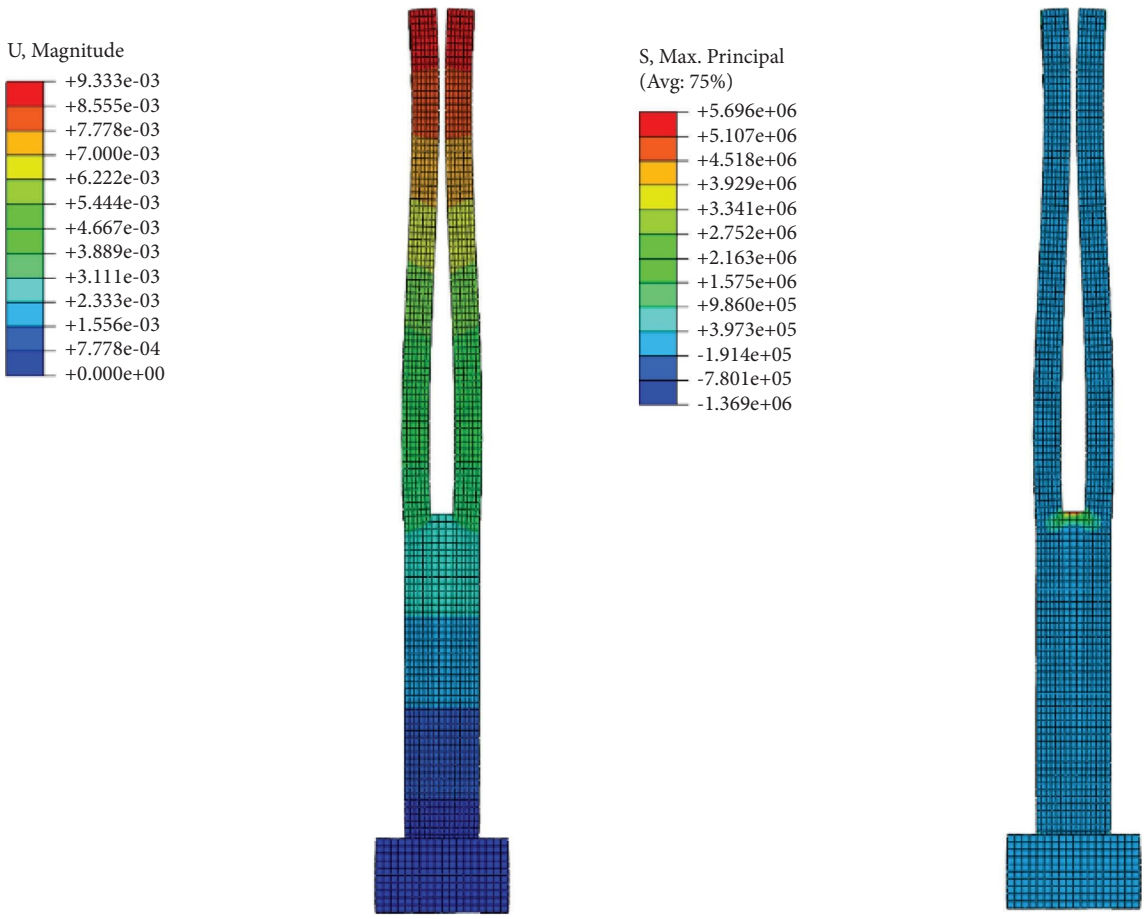

Figure 16: Deformation diagram of double-leg thin-walled piers under anchorage removal.

rigid frame bridge and reduce the additional internal force of the bridge. However, due to the existence of the tensile stress on the inside of the single limb, the pier will crack if it is not handled properly, so local reinforcement must be done when this type of pier is used.

3.3. Applying Seismic Time-History Load. The seismic area where the bridge is located is 8 degrees, the site is class III, the design reference period is 100 years, and the substructure and special position of the bridge are the key fortification parts. In order to simulate the seismic time-history load, based on the data of PEER (Pacific earthquake Engineering Research Center), the processed waveforms of seismic waves occurring near this area are obtained as shown in Figure 17:

When the earthquake intensity is lower than the earthquake intensity, the destructive effect of the frequent earthquake on the bridge structure is small. The acceleration of the common earthquake is 0.08 g and the gravity acceleration is defined as gravity acceleration. For the convenience of the study, the safe value is 10 m/s^2, and the peak value of seismic acceleration is within 0.8 m/s^2.

In this paper, on the basis of the time-history analysis of the common earthquake of the connecting pier, the time-history analysis is also done under the action of rare earthquake. The seismic wave used is the seismic wave obtained after amplification and correction of common seismic waves, and the peak seismic acceleration reaches 4 m/s^2, as shown in Figure 18.

Under the stress state after the analysis of the ABAQUS construction stage, the model applies the acceleration time-history load in three directions: common earthquake and rare earthquake, carries on the time-history analysis, and obtains the time-history analysis result data.

3.4. Force Analysis Based on Rain Flow Counting Method. In the vertical direction of the double-leg thin-walled pier, the maximum principal stress data of three elements (as shown in the figure) are calculated by using the rain flow counting method, and the stress interval, average stress and cycle times can be obtained, as shown in Figure 19. The rain flow method is regarded as the most common cycle-counting method used in the irregular loading spectrum and is therefore adopted in this study [7].

As shown in Figure 20, from the statistics of the rain flow count of the maximum principal stress in frequently encountered earthquakes, the maximum principal stress at position 1 and 3 of the connecting pier is larger, and the stress at position 2 is smaller, and the average stress of the maximum cycle number of the element at position 1 is about 2.9 MPa, the element at position 2 is about 1.24 MPa, and

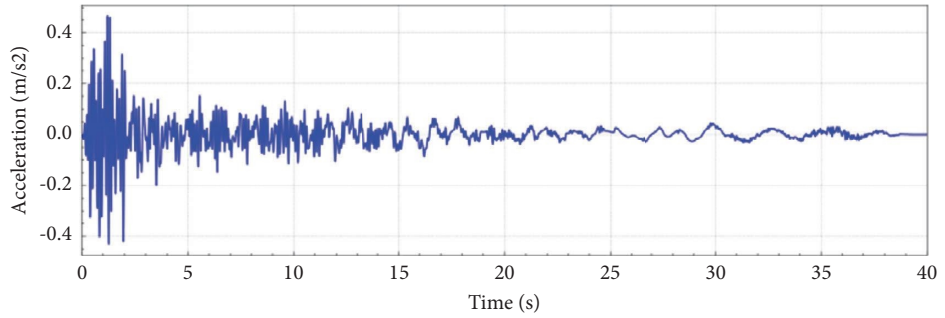

(a)

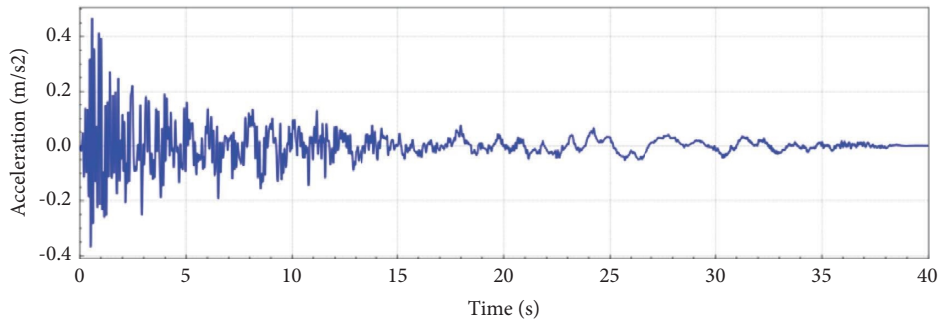

(b)

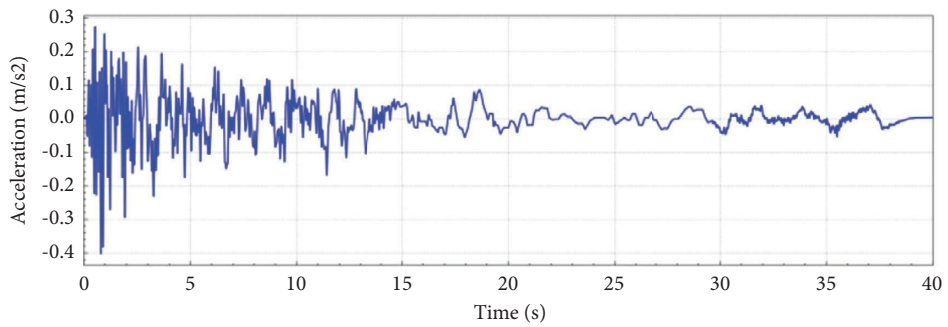

(c)

Figure 17: Frequently encountered seismic waves. (a) N-S seismic wave. (b) E-W seismic wave. (c) U-D seismic wave.

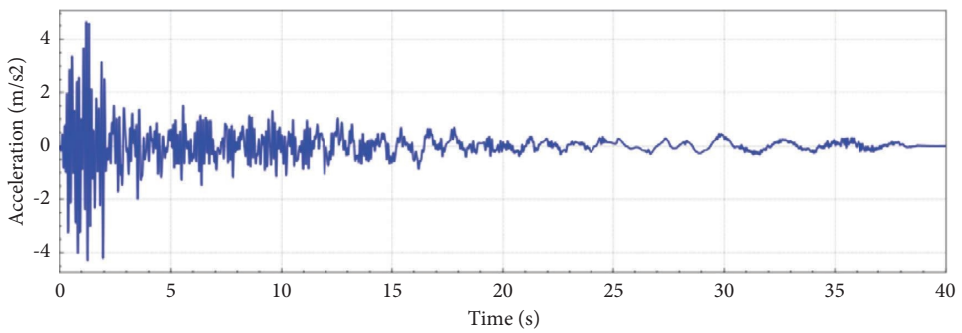

(a)

Figure 18: Continued.

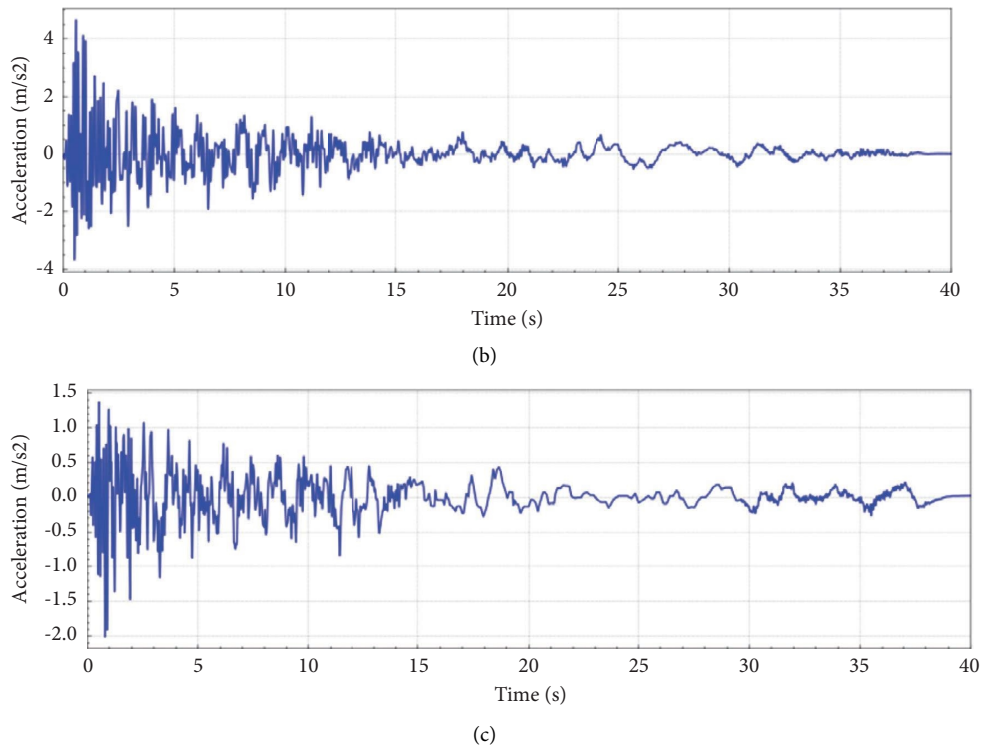

Figure 18: Rare seismic waves. (a) N-S seismic wave. (b) E-W seismic wave. (c) U-D seismic wave.

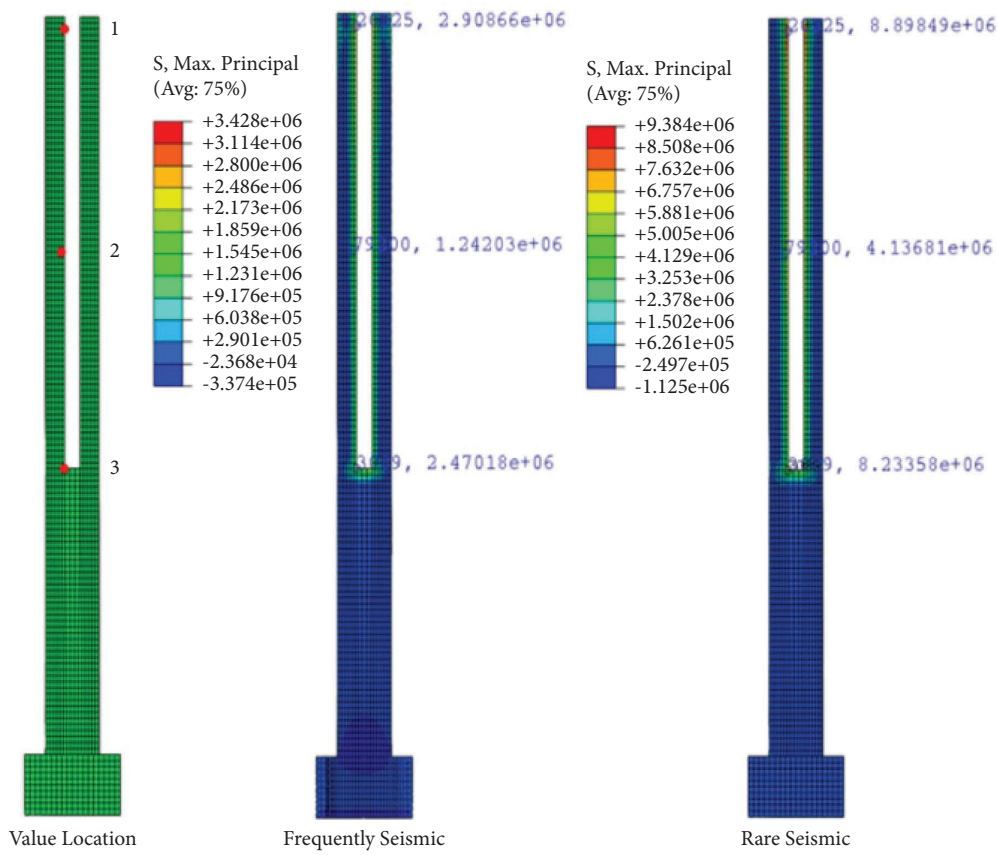

Figure 19: Calculation results of seismic spectrum.

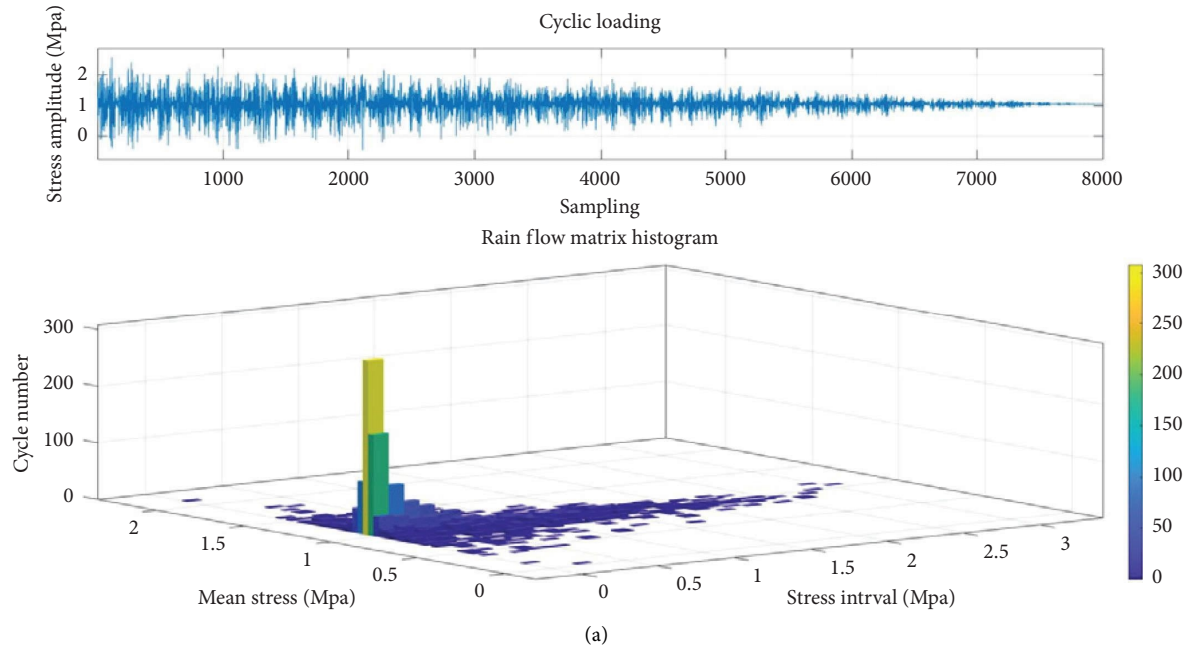

(a)

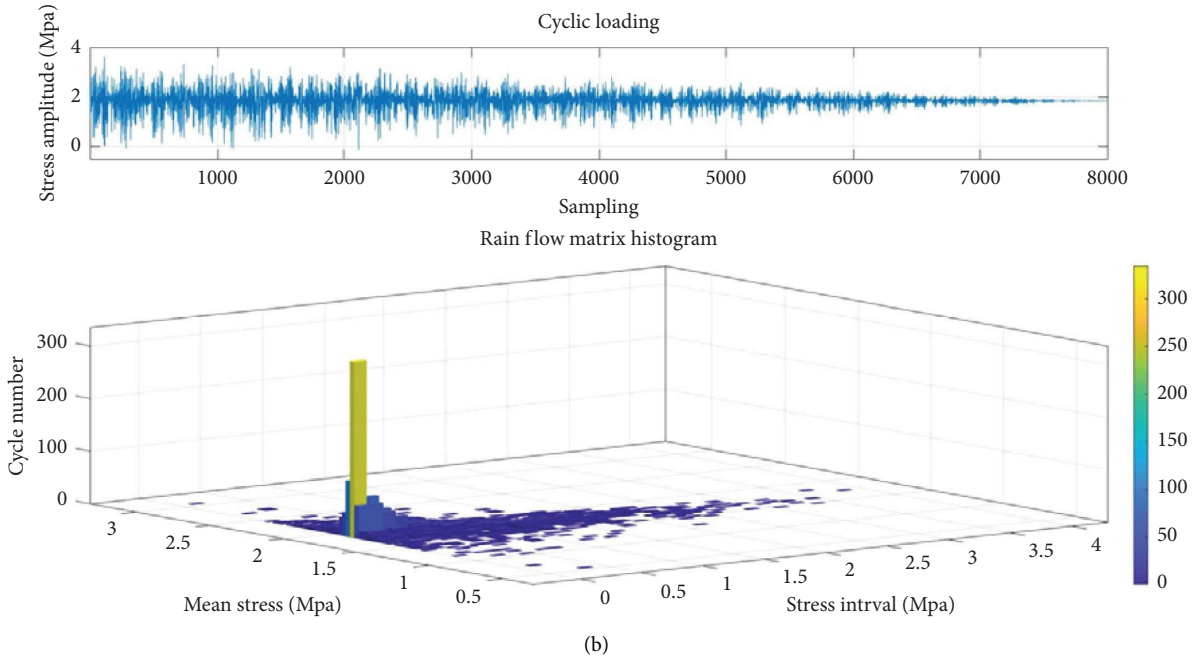

(b)

Figure 20: Continued.

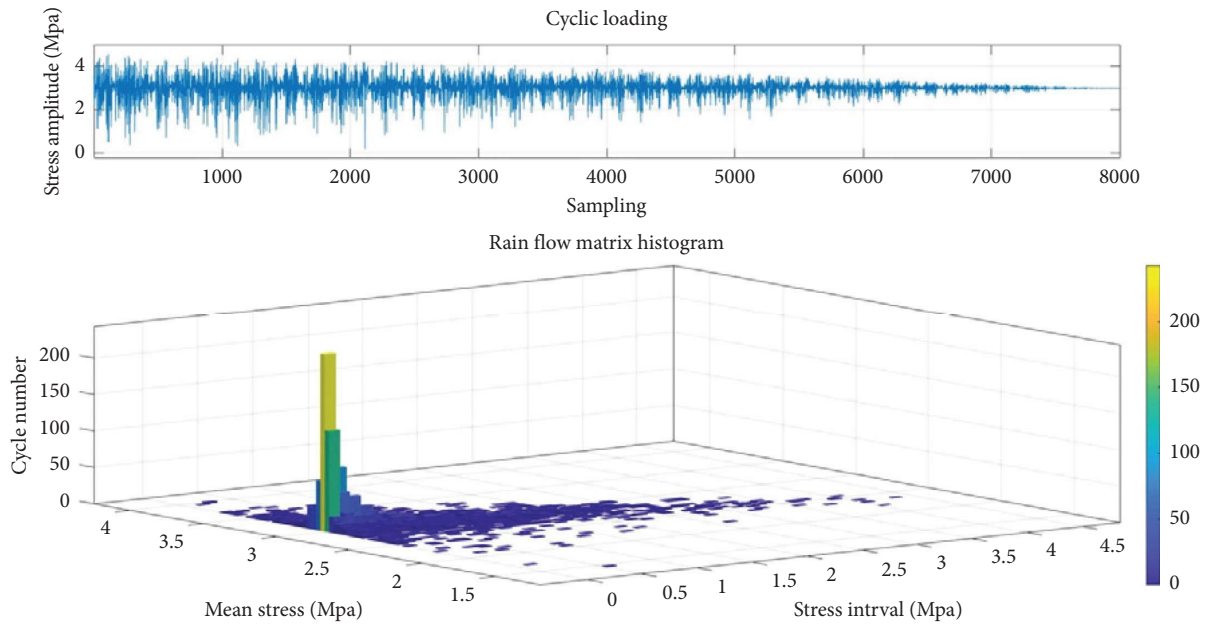

(c)

Figure 20: Statistics of rain flow count of maximum principal stress in frequently encountered earthquake units. (a) Rain flow count statistics of units at location 1. (b) Rain flow count statistics of units at location 2. (c) Rain flow count statistics at 3 locations.

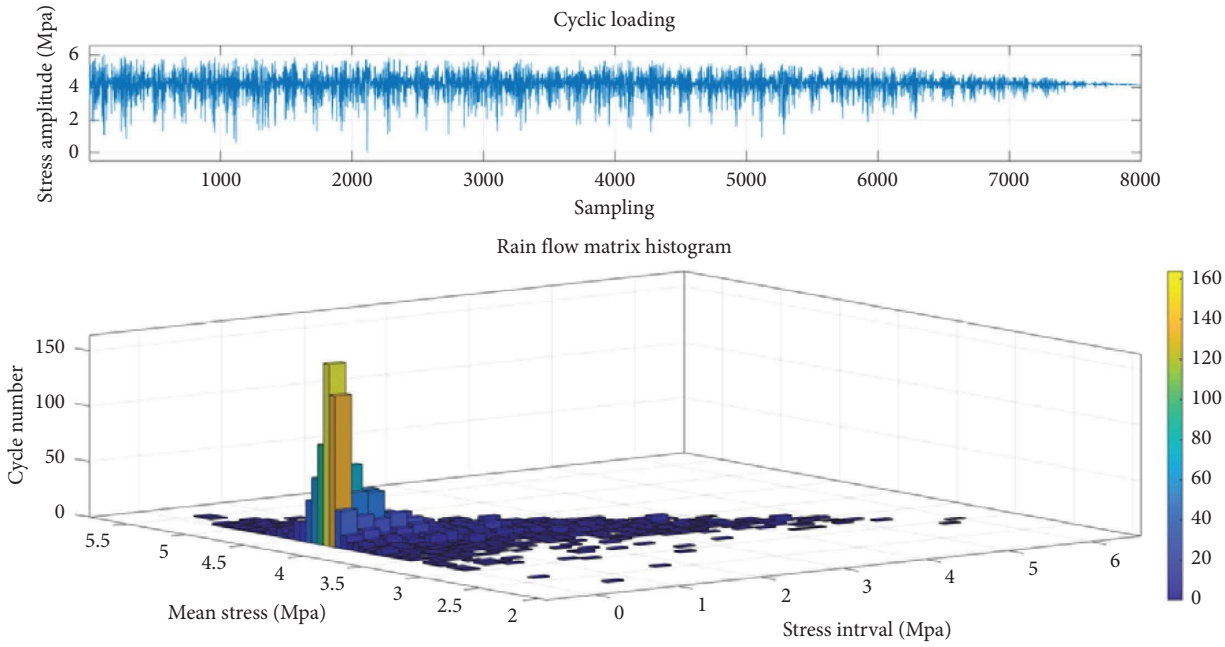

(a)

Figure 21: Continued.

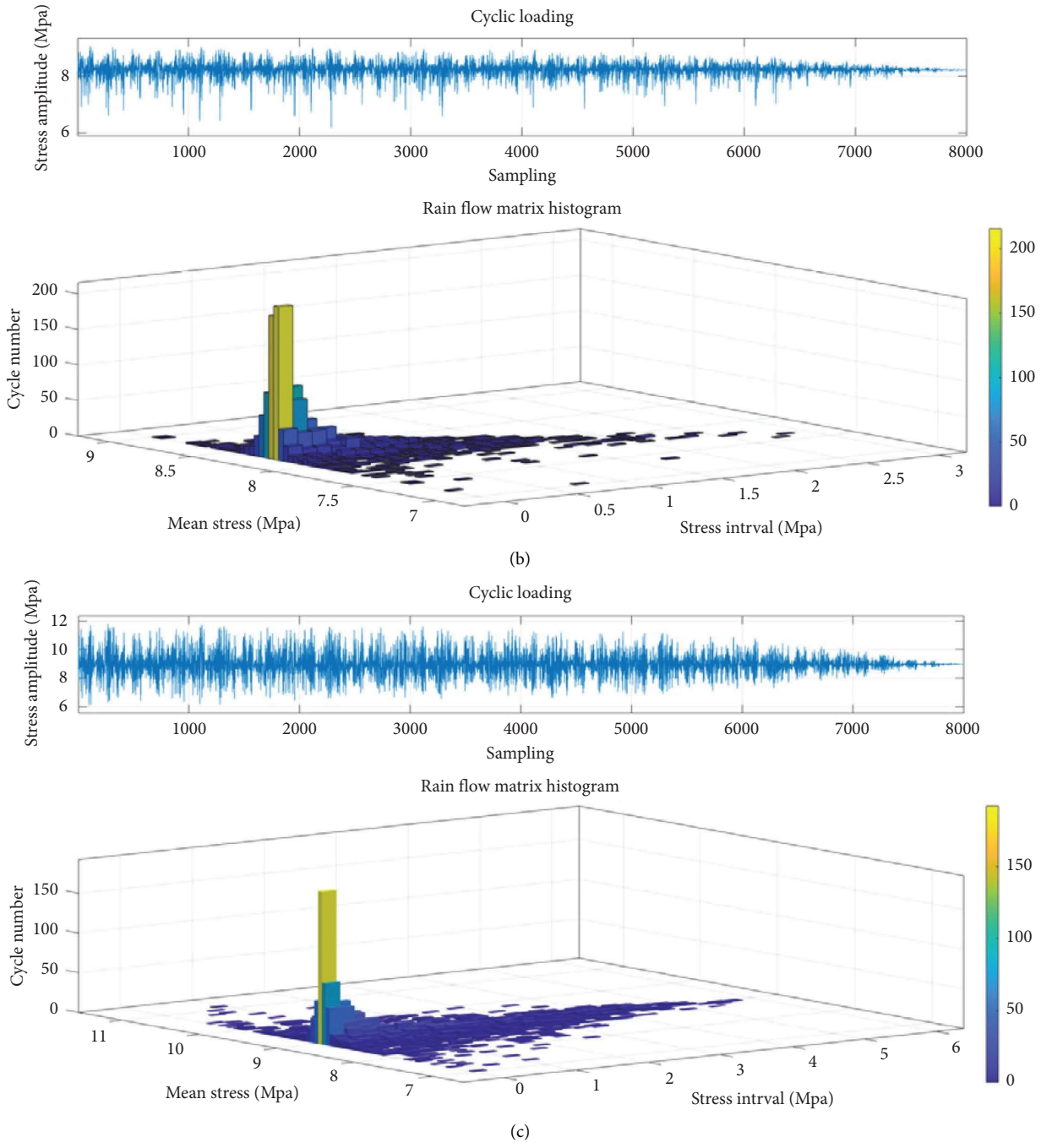

Figure 21: Statistics of rain flow count of maximum principal stress in rare earthquake units. (a) Rain flow count statistics of units at location 1. (b) Rain flow count statistics of units at location 2. (c) Rain flow count statistics at 3 locations.

that at position 3 is about 2.47 MPa, so under the action of common earthquakes, the concrete on the surface of the two limbs of the connecting pier will not produce structural cracks, and the pier can work normally.

As shown in Figure 21, from the rain flow count statistics of the maximum principal stress of rare earthquakes, the distribution law of the maximum principal stress is similar to that of common earthquakes, but the value of principal stress increases greatly. The stress average value of the maximum cycle number of the element at location 1 is about 8.9 MPa, the element at location 2 is about 4.1 MPa, and the element at location 3 is about 8.23 MPa. The concrete on the surface of

both limbs of the connecting pier has been cracked, and the internal steel bar will play an important role in the bearing capacity.

4. Conclusion

The approach bridge of Quanzhou Bay Bridge on Fuzhou-Xiamen High-speed Railway is a multijoint rigid frame bridge without support. The top of the transfer pier is broken horizontally along the bridge, and the large deformation capacity of the double-limb thin-walled flexible pier can effectively release the deformation of the multijoint due to temperature change and other factors. In order to adopt the same cantilever cast-in-place construction technology as the middle pier in the construction, the zero block separated from the pier is temporarily anchored to form a whole, and the temporary anchorage is removed after the cantilever construction is closed.

Due to the complex force of the construction method, the bridge structure will undergo structural system transformation, so it is necessary to analyze the mechanical state of related components in the process of construction and system transformation in detail. In this paper, through the establishment of a high authenticity finite element model, the deformation and stress changes of the junction pier in each construction stage are calculated and analyzed, and its mechanical laws are summarized, so as to provide a reference for the future application of this type of pier.

Data Availability

The data used to support the findings of this study are included within the article.

Conflicts of Interest

The authors declare that they have no conflicts of interest.

Acknowledgments

This project was supported by the science and technology research and development plan of China Railway Corporation_K2018G017.

References

[1] X. Yang, F. Lin, and M. Huang, "Analysis of the law of joint deformation for grouted mortise-tenon joint," *Advances in Civil Engineering*, vol. 2022, Article ID 2909993, 13 pages, 2022.

[2] S. Mostafa Mousavi, B. Ataie-Ashtiani, and S. Mossa Hosseini, "Comparison of statistical and mcdm approaches for flood susceptibility mapping in northern Iran," *Journal of Hydrology*, vol. 612, 2022.

[3] H. Guo, D. Zhou, and Y. He, "Trajectory control algorithm of flexible joint manipulator based on random matrix and screw theory," *Mathematical Problems in Engineering*, vol. 2022, Article ID 6073374, 12 pages, 2022.

[4] C. Lesmana, H.-T. Hu, T.-C. Pan, and Z.-S. Lin, "Parametric study on nonlinear finite element analysis of prestressed reinforced concrete beam strengthened by fiber-reinforced plastics," *Mathematical Problems in Engineering*, vol. 2022, Article ID 9646889, 11 pages, 2022.

[5] J. Jia, J. Gao, W. Wang, L. Ma, J. Li, and Z. Zhang, "An automatic generation method of finite element model based on bim and ontology," *Buildings*, vol. 12, 2022.

[6] H. Zhao, Y. Ding, S. Nagarajaiah, and A. Li, "Longitudinal displacement behavior and girder end reliability of a jointless steel-truss arch railway bridge during operation," *Applied Sciences*, vol. 9, no. 11, p. 2222, 2019.

[7] W. Meng, L. Xie, Y. Zhang, Y. Wang, X. Sun, and S. Zhang, "Effect of mean stress on the fatigue life prediction of notched fiber-reinforced 2060 Al-Li alloy laminates under spectrum loading," *Advances in Materials Science and Engineering*, vol. 2018, Article ID 5728174, 16 pages, 2018.